Vibration Testing

B.J. Rebollo, C.W. Keer, D.D. Avant, J.B. Czarnecki

Charles Keer

Blake Rebollo

Devin Avant

Jacob Czarnecki

Embry-Riddle Department of Aerospace Engineering
Embry Riddle Aeronautical University, Daytona Beach, Florida
April 2023

Table of Contents

Table of Figures

Table of Tables

Abstract

Using vibration testing, two aluminum beams were tested under various frequencies to determine resonance. Strobe illumination was used to hone and visually identify resonant frequencies and corresponding harmonics along with an accelerometer connected to an oscilloscope to visualize the data. It was found that the aluminum beams resonated at different frequencies and harmonics which were functions of the beam length. By increasing the frequency, the number of nodes went up as the beam resonated faster. Additionally, an aircraft part was tested till its first mode of resonance to illustrate a real-world example.

Introduction

It is widely recognized that load-bearing structures, when subjected to excessive static loads, can experience failure. This is a well-known phenomenon in engineering and is often taken into consideration in the design and construction of structures. However, it is important to note that structural failure can also occur at much lower load levels when the right type or combination of disturbances are applied. For instance, when structures are subjected to continuous or periodic loading at frequencies near their resonance frequencies, they can experience large displacements and even catastrophic failure if not adequately planned for.

Resonance frequencies are specific frequencies at which a structure vibrates with the maximum amplitude in response to external forces. These frequencies depend on various factors, including the shape of the structure, its material composition, attachment methods, excitation, damping, and other complex interactions, which can make predicting and simulating resonance behavior challenging. Resonance frequencies are an important aspect of vibration testing in engineering because they can significantly impact the behavior and response of structures to external disturbances.

To better understand the conditions that can lead to the loss of structural integrity or resonance, structural vibration testing is often employed. In this approach, the structure under investigation is instrumented with sensors to measure its response to externally applied disturbances. Known disturbances are then applied to the structure, and its dynamic response is carefully measured and observed, including the amplitudes of vibrations. If the structure exhibits excessive displacements or other signs of instability at certain frequencies, it may indicate the presence of resonance, which can potentially lead to structural failure if not addressed.

In aerospace engineering, understanding and managing resonance frequencies are crucial for ensuring the structural integrity and reliability of aircraft and spacecraft. Aerospace Engineers, especially those focused on Astronautics, need to understand this phenomenon due to excessive vibration present into aircraft and spacecraft operations, compared to other engineering disciplines. Resonance frequencies can have significant effects on the dynamic behavior and response of aerospace structures, and failure to properly account for them can result in catastrophic consequences, such as structural damage or even complete structural failure during operation. Vibration testing is a crucial aspect of aerospace engineering as it helps ensure the safe and reliable

operation of aerospace structures, systems, and components. Here are some specific reasons why vibration testing is important in aerospace engineering.

The goal of structural vibration testing is to experimentally identify and study the conditions that can cause failure or resonance in structures subjected to forced disturbances. This helps engineers and researchers gain insights into the behavior of structures under different loading conditions, and aids in the development of improved design strategies to prevent unexpected structural failures. By studying the dynamic response of structures under controlled testing conditions, engineers can better understand how a structure's performance may be affected by external disturbances and make informed decisions in the design and construction phases to ensure structural integrity and safety.

For this experiment, two main pieces of equipment were used. One of the key tools in vibration testing is an Electrodynamic Shaker. This is a device that converts controlled electrical current into dynamic mechanical force, providing test engineers with a versatile range of vibration testing possibilities. These devices, commonly known as shakers, are capable of simulating three fundamental types of test environments: sine, random, and shock testing. They are controlled by signal generators that can be set to desired test conditions. Vibration tests conducted using these shakers are crucial for verifying the quality, reliability, and stability of structures subjected to dynamic loads. Additional equipment such as cooling fans, signal generators, accelerometers, oscilloscopes, and stroboscopes are often used to complete the vibration testing setup.

The second key piece of equipment used for this lab was a digital stroboscope. This is a device that emits regular flashes of intense light. In the context of studying motion, a rapidly flashing strobe light can create an effect where periodically moving objects appear to come to a stop, such as rotating machinery or periodic vibrations. These strobes are designed to have a high flash energy that can discharge in a matter of milliseconds or even less, making them extremely bright. Typically, the light source in a strobe is a xenon gas flash lamp. To generate a quick and brilliant flash, a high voltage source, usually stored electric charge in a capacitor, is rapidly delivered to the gas upon triggering. As the current passes through the gas-filled tube, the xenon electrons become excited and jump to higher energy levels, then rapidly drop back down, releasing photons (light) in the process.

In a vibration test, the shaker simulates various types of vibrations, such as sine waves, random vibrations, or shocks, depending on the desired test conditions. By applying known vibrations to the test object, the shaker allows the test engineer to study the response of the object and evaluate its structural integrity, reliability, and stability. The stroboscope is used to visually observe the motion or behavior of the test object. The rapid flashes of light from the stroboscope creates an effect where moving objects appear to come to a stop or slow down, allowing the test engineer to study the object's motion or behavior more closely.

For the sake of the lab we conducted, the main objectives were to learn how to set up and use vibration equipment to agitate and test engineering structures, observe natural decay in underdamped structures, and gain an appreciation for dynamic structural behavior and compare experimentally observed natural frequencies and node locations to model predictions.

Equipment

1.Al-6061-T651 beam samples (1 Long and 1 Short) and aircraft structural part form Boeing 787.

2.Screws, washers, tube spacers, and Phillips head screwdriver

3.Calipers, ruler and tape measure

4.Whiteboard markers

5.ICP® (integrated-circuit piezoelectric) accelerometer and signal conditioner

6.Hot glue and gun

7.Digital oscilloscope (V and s)

8.Power supply amplifier

9.Electrodynamic shaker and cooling fan

10.Sweep sine generator(cycle/s)

11.Digital stroboscope(flash/min) and tripod

12.Various wires, cables, and connectors

13.Power supply strip and possibly extension cord

Methodology

1. The accelerometer was attached to the shaker piston hole using hot glue, connected to the signal conditioner, and then to the oscilloscope.

2. The power supply strip was turned on to power up the signal conditioner and oscilloscope

3. The oscilloscope was reconfigured by: Resetting to default settings, using auto setup, and setting voltage and time settings to about 20mV/div and 50ms/div as a starting point, and adjusting these values later to match the amplitude and frequency.

4. The short beam sample was selected, and its cross section was measured.

5. The beam sample was connected to the shaker table piston in a cantilever beam arrangement using 2 tube spacers, 2 screws, and 4 washers. The washers were positioned on top and bottom of the beam, with the smoothest edges touching the beam to prevent fatigue crack initiation. The tube spacers kept the beam sample elevated above the piston.

6. The distance from the free end of the beam sample to the closest tube spacer was measured and recorded as the beam length.

Figure 1. Calibrating shaker table controls.

Figure 2. Attaching beam to shaker table.

7. The 5530 Power Supply amplifier was configured by: Turning the Channel 1 knob (amplitude) all the way to the left, and the Channel 2 knob (nothing) all the way to the left.

8. The sweep sine generator was set up by: Turning the frequency knobs all the way to the left, turning MANUAL mode on, and turning on other checked buttons.

9. The 5530 Power Supply Amplifier was turned on using the switches on the rear and front.

10. The control frequency FINE knob on the sweep sine generator was adjusted to about its midpoint. The COARSE knob was slowly adjusted to cause structural resonance and other desired responses. Lastly, the FINE knob was used for more delicate control. The amplitude was adjusted gently and conservatively, as very little amplitude is needed.

For the Flashing light sensitivity section:

1.Turned off the overhead room lights and observed resonance (in slow motion) using the digital stroboscope with flash adjusted appropriately.

2.Noted that the sweep sine generator displayed cycle/s (Hz) while the stroboscope displayed flash/min.

3.Monitored and recorded the excitation frequencies as indicated by the control frequency setting, digital stroboscope, and oscilloscope. For frequencies less than a few Hz, the low-frequency signal may not have been very clear on the oscilloscope.

4.Adjusted the V/div and time/div settings of the oscilloscope to allow clear observation of the major wave period (e.g., time from peak to peak).

5.Inverted this to get the major frequency or read it from the oscilloscope display if available for frequencies above 10 Hz.

6.Tried auto setup → Auto Set again if desired.

7.Made a few sketches and/or took photographs of the seemingly slowed motion and nodes of potential interest.

8.Marked/measured/recorded the node positions using a whiteboard marker and ruler. Periodically checked to make sure the screws were tight.

9.Repeated the above procedure for the long beam sample.

10.Lastly, consider vibrating real aircraft parts (e.g., hat-shaped, leading-edge rib, etc.). When finished, turned the amplitude and frequency way down, turned off the 5530 Power Supply Amplifier, other components, and lastly, the power supply strip. Cleaned up. Made copies of the test data, observations, and other pertinent information.

Results

The critical dimensions of the two aluminum beams were measured and tabulated in Table ##. Each mode and corresponding measurements were also tabulated for each test. The nodes of each peak in the aluminum were measured once the strobe light indicated that the aluminum was not out of frequency from the strobe.

Table 1. Beam Critical Dimensions.

Beam Dimensions	L (cm)	B (mm)	H (mm)
Short	77.1	25.43	4.77
Long	128.3	25.1	4.94

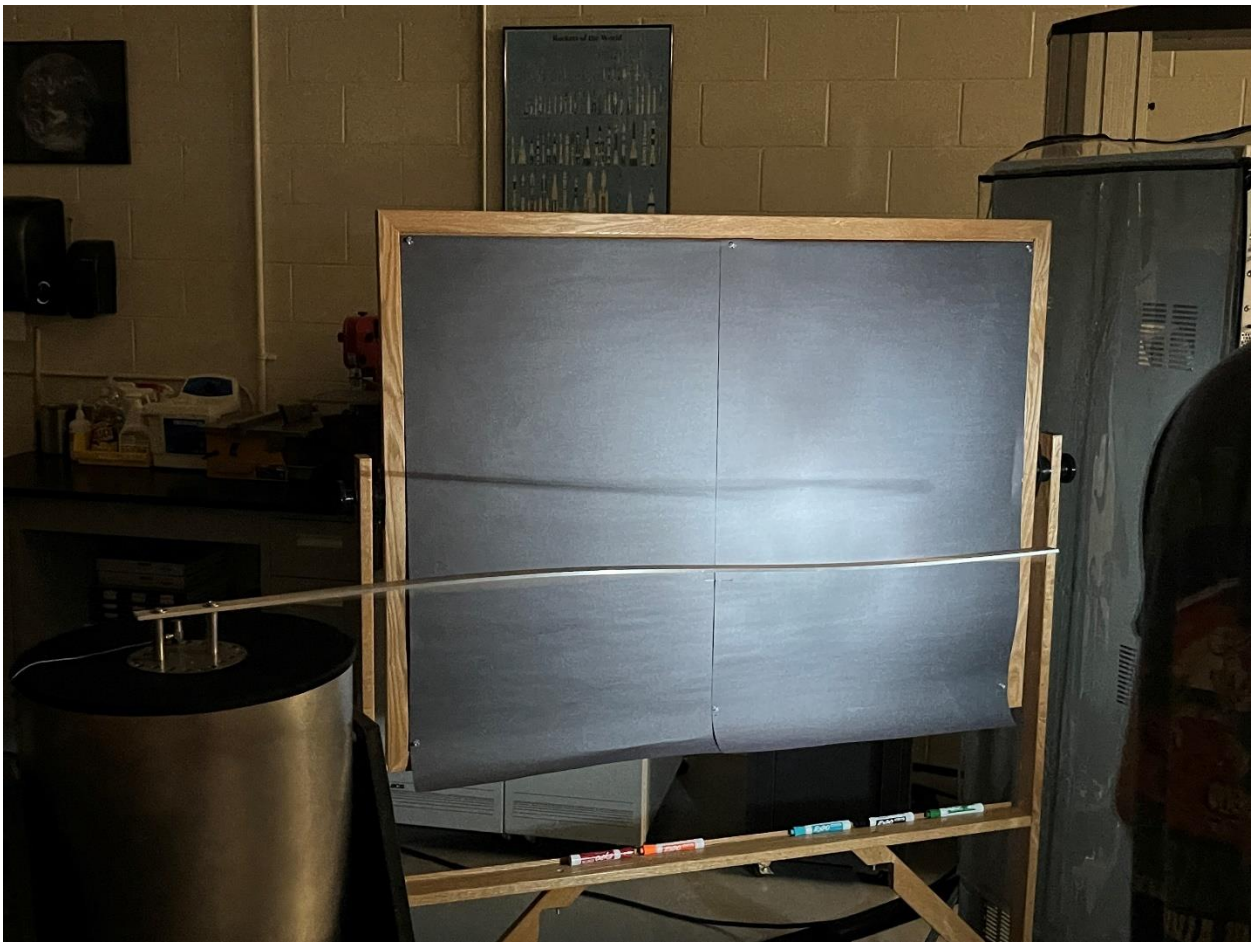

Figure 3. Example of beam in Mode 2 under strobe.

Table 2. Short beam modes and frequency measurements.

Short	Fssg (Hz)	Fpo(Hz)	Fstrobe (fpm)	Node 1 (cm)	Node 2 (cm)	Node 3 (cm)
Mode 1	6.1	6.078	369	-	-	-
Mode 2	38.5	38.46	2310	59.8	-	-
Mode 3	107.6	107.65	6455	37.7	66.8	-

Table 3. Long beam modes and frequency measurements.

Long	Fssg (Hz)	Fpo (Hz)	Fstrobe (fpm)	Node 1 (cm)	Node 2 (cm)	Node 3 (cm)
Mode 1	2.4	2.38	140	-	-	-
Mode 2	14.6	14.49	877	99.5	-	-
Mode 3	40.7	40.65	2445	62.9	110.7	-
Mode 4	80	80.65	4803	43.8	81.4	115.4

Figure 4. Strobe setup with recording camera.

Discussion

To perform an analysis on the experimental results, we will have to compare them to the theoretical values for frequency obtained by classical calculations. To find the natural frequency of the part we will have to use Eq. 1. The variables needed to solve this have been obtained using the dimensions of the part, as well as the given eigen values. The frequency used is recorded by an oscilloscope. The material of the beam is 6061 Al. This means it has a Youngs Modulus of 68.9 GPa as well as a density is 2720 kg/m3.

$$\omega_n = \frac{(\lambda_n L)^2}{L^2}\left(\frac{EI}{\rho A}\right)^{\frac{1}{2}} \quad (1)$$

$$I = \frac{bh^3}{12} \quad (2)$$

$$f = \frac{\omega_n}{2\pi} \quad (3)$$

Table 4. Eigenvalues for each case.

Case	Eigen value
$\lambda_1 L$	1.8751
$\lambda_2 L$	4.6941
$\lambda_3 L$	7.8547
$\lambda_4 L$	10.9956

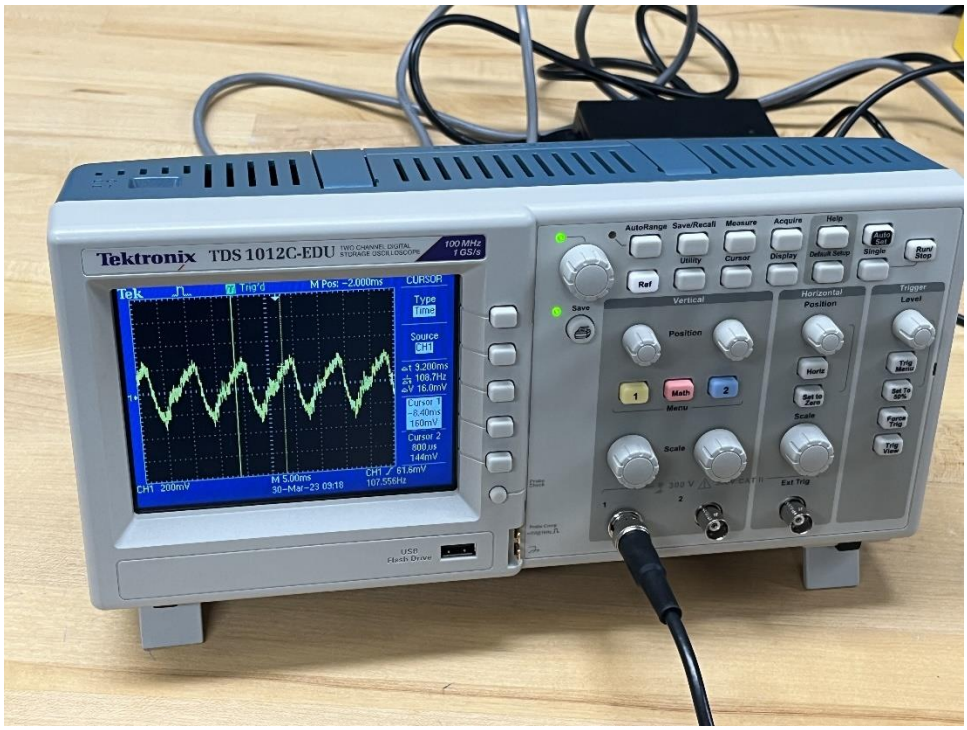

Figure 5. Oscilloscope at 107.56 Hz from accelerometer attached to shaker table.

For each Mode, the percent difference was found for each case for the strobe, accelerometer and oscilloscope, and the reading on the shaker table. It was found that strobe had the lowest percent

difference from the indicated frequency on the shaker table, meaning that it was the most accurate form to confirm the resonant frequency. Each measurement was within 7%, which, while large, is understandable given the nature of the test. This test required that the beam not "move" while under strobe, indicating the strobe has matched the resonant frequency. This visual test has inherent user error and will be a few percent higher than a more precise measurement. Additionally, the data being consistently different by ~6% indicates that the calibration on the shaker table may be slightly off on the digital readout.

Table 5. Short beam resonant frequencies.

Case	f
Mode 1	6.52
Mode 2	40.89
Mode 3	114.48

Table 6. Long beam resonant frequencies.

Case	f
Mode 1	2.44
Mode 2	15.29
Mode 3	42.8
Mode 4	83.87

With the values for theoretical frequency calculated for each mode, they could be compared to each of the three experimental values for each mode. The method to doing this was finding the percent difference between each. The percentage differences were calculated for both long and short beams. Interestingly, the short beam yielded a greater percent difference than the long beam. The short beam difference would average ~6% whereas the long beam was ~4%. This may have been due to the shorter beam having a higher frequency as there may be a drop in precision in our equation for omega. The only significant change in the omega calculation from the short and long beam was the length, which is most definitely accurate.

Table 7. Short beam theoretical frequencies and % difference.

	Mode 1 % Diff	**Mode 2 % Diff**	**Mode 3 % Diff**
Fssg	6.44%	6.21%	6.39%
Fpo	6.78%	6.32%	6.34%
Fstrobe	5.84%	6.02%	6.21%

Table 8. Long beam theoretical frequencies and % difference.

	Mode 1 % Diff	**Mode 2 % Diff**	**Mode 3 % Diff**	**Mode 4 % Diff**
Fssg	1.67%	4.73%	5.16%	4.84%
Fpo	2.49%	5.37%	5.15%	3.91%
Fstrobe	4.61%	4.48%	4.91%	4.66%

The data collected from the experimental values such as Fssg, Fstroke, and Fpo were also compared between each other for Mode 1 of both the short and long beam experiments. The percentage differences shown between each other are significantly smaller than the percentage differences between them and the theoretical frequency values of Mode 1. The difference percentage was within 1% of each other. This gives a level of credibility to all three experimental procedures as the data collected was consistent with one another.

Table 9. Mode 1 comparison and % difference of short beam.

	Fssg	**Fpo**	**Fstrobe**
Fssg	-	0.36%	0.82%
Fpo	0.36%	-	1.18%
Fstrobe	0.82%	1.18%	-

Table 10. Mode 1 comparison and % difference of long beam.

	Fssg	**Fpo**	**Fstrobe**
Fssg	-	0.1%	0%
Fpo	0.1%	-	0.1%
Fstrobe	0%	0.1%	-

Table 11. Short beam node % difference.

	Node 1 Measured (cm)	**Node 1 Theoretical (cm)**	**Node 2 Measured (cm)**	**Node 2 Theoretical (cm)**	**% Difference Node 1**	**% Difference Node 2**
Mode 2	59.8	60.36	~	~	0.93	~
Mode 3	37.7	38.86	66.8	66.92	1.16	0.12

Table 12. Long beam node % difference

	Node 1 Measured (cm)	Node 1 Theoretical (cm)	Node 2 Measured (cm)	Node 2 Theoretical (cm)	Node 3 Measured (cm)	Node 3 Theoretical (cm)	% Difference Node 1	% Difference Node 2	% Difference Node 3
Mode 2	99.5	100.45	~	~	~	~	0.95	~	~
Mode 3	62.9	64.66	110.7	111.36	~	~	2.76	0.59	~
Mode 4	43.8	45.93	81.4	82.63	115.4	116.24	4.75	1.50	0.73

The node percent difference was found using the length of the measured node from the connection point to the location of the standing wave on the beam as well as the calculated theoretical value. Mode 1 was not calculated since there are no node locations on the beam. Mode 4 was measured only for the long beam. By using the eigenvalues and the length of the beam, a fractional location was found where each standing node would be located at any frequency. Comparing this to the measured values yields relatively high confidence in these measurements as can be seen in Table 11 and Table 12.

Conclusion

In conclusion, the vibration testing lab showed how the tested Aluminum vibrated at different resonant frequencies. Being able to visually see how the aluminum beams vibrated at their resonate frequencies allowed us to gain an appreciation for the importance of vibration testing on materials and structures used for aerospace applications. By utilizing both the oscilloscope and the digital stroboscope to analyze the resonate frequencies, and comparing the results they gave, we saw relatively low percentage differences. The digital stroboscope produced the smallest percentage differences when compared to the theoretical values for the short beam, which could be contributed to its ease of setup and use compared to the other methods, leaving less room for error.

References

Aggarwal, P. K. (n.d.). *Dynamic (Vibration) Testing: Design-Certification of Aerospace System*.

Embry-Riddle Aeronautical University Department of Aerospace Engineering, AE 417 Lab Bulletin 5: *Vibration Testing*

Inman, D. J. (2009). *Engineering vibration*. Pearson/Prentice Hall.

McConnell, K. G., & Varoto, P. S. (2008). *Vibration testing: Theory and practice*. Wiley.

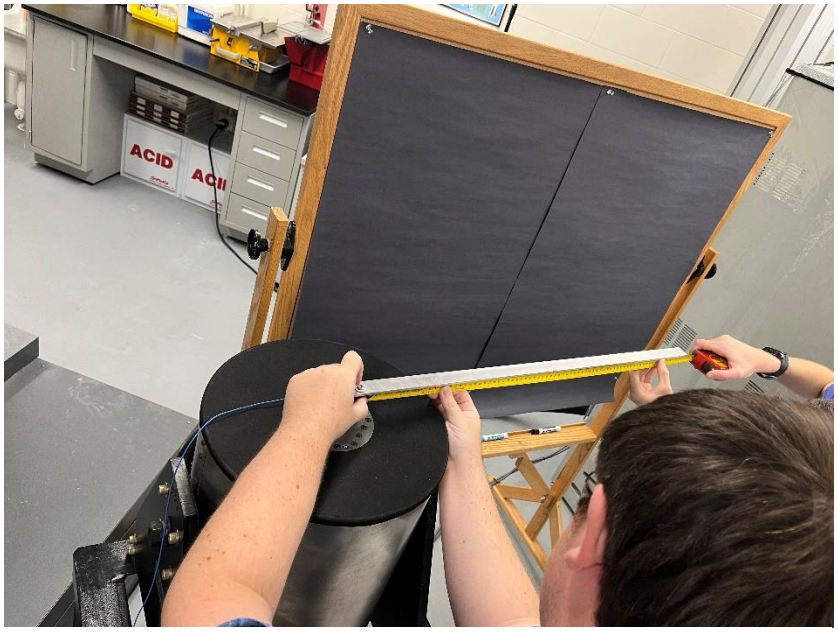

Figure 6. Measuring beam from attachment point.

Appendix

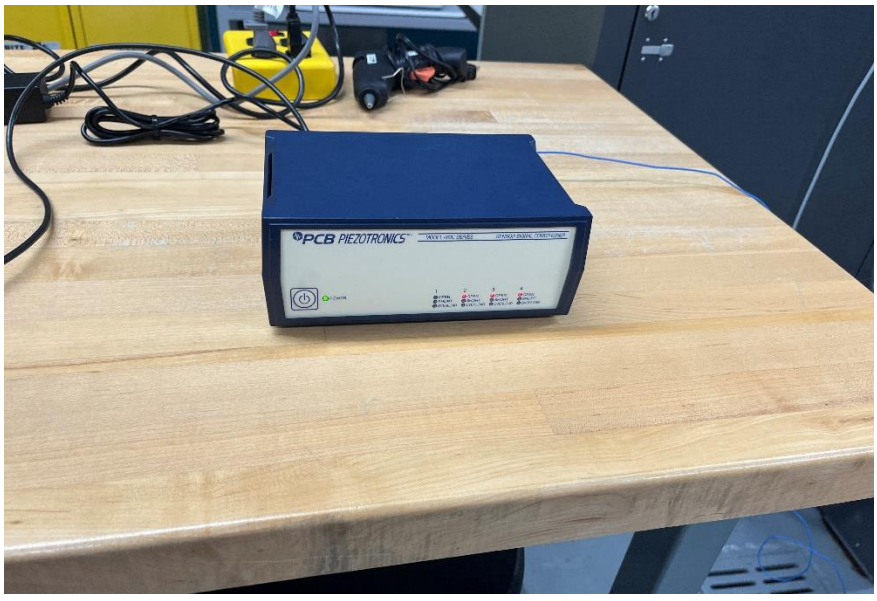

Figure 7. ADC for accelerometer

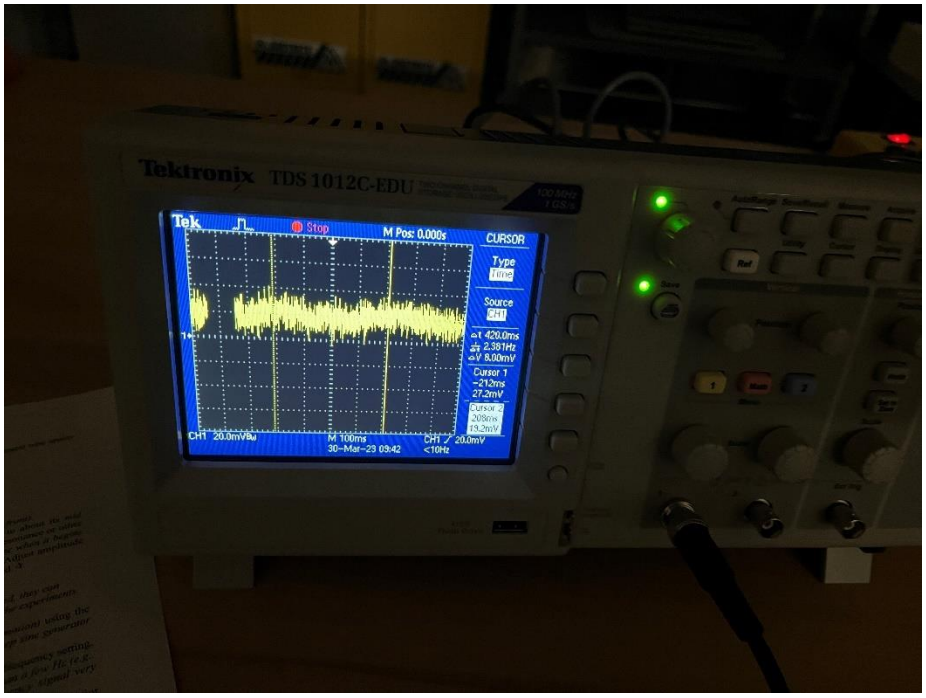

Figure 8. Example oscilloscope calculation for first mode on long beam.